Supplemental information

Autonomous Humidity Regulation by MOF/Wood Composites

Kunkun Tu [1,2,3 #], Zhidong Zhang [4 #], Christopher H. Dreimol [3,5], Roman Günther [6,7], Robert Zboray [8], Tobias Keplinger [3,9], Ingo Burgert [3,5], Yong Ding [3,5]*

[1] *Jiangsu Key Laboratory of Coal-based Greenhouse Gas Control and Utilization, China University of Mining and Technology, Xuzhou, Jiangsu, 221008, China*

[2] *Carbon Neutrality Institute, China University of Mining and Technology, Xuzhou, Jiangsu, 221008, China*

[3] *Wood Materials Science, Institute for Building Materials, ETH Zürich, 8093, Zürich, Switzerland.*

[4] *Durability of Engineering Materials, Institute for Building Materials, ETH Zurich, 8093 Zurich, Switzerland*

[5] *WoodTec Group, Cellulose & Wood Materials, Empa, 8600 Dübendorf, Switzerland*

[6] *Laboratory of Adhesives and Polymer Materials, Institute of Materials and Process Engineering, Zurich University of Applied Sciences, 8401 Winterthur, Switzerland*

[7] *Laboratory for Multifunctional Materials, Department of Materials, ETH Zürich, 8093 Zürich, Switzerland*

[8] *Center for X-ray Analytics, Empa, 8600 Dübendorf, Switzerland*

[9] *AgroBiogel, 3430 Tulln, Austria*

[#] *These authors contributed equally*

* *Corresponding author:*

yoding@ethz.ch

1. Characterization of MOF/wood composites

1.1 Comparison of humidity regulation performance of MOFs and other porous materials.

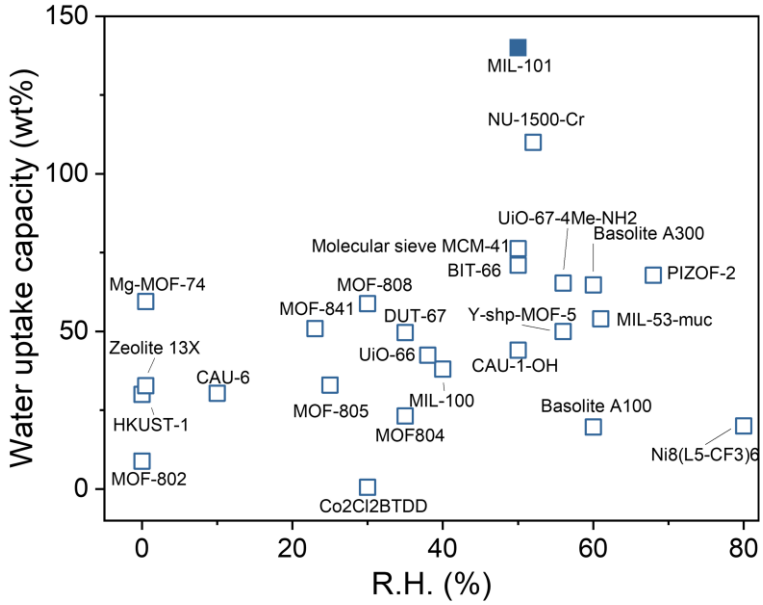

Figure S1 Comparison of water adsorption capacity and desorption trigger points between as-synthesized MOFs and representative water-adsorbing porous materials.

1.2 Synthesis and characterization of MOF.

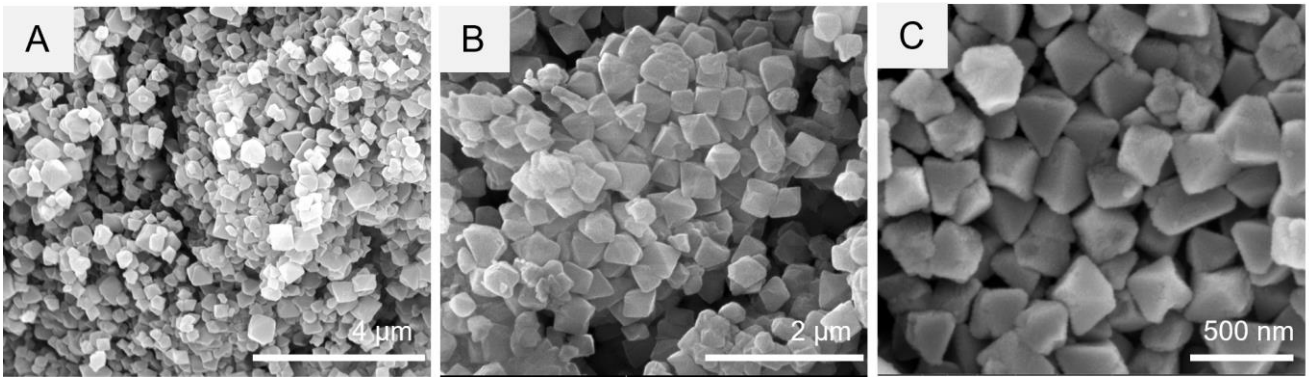

Figure S2 SEM images of synthesized MIL-101(Cr).

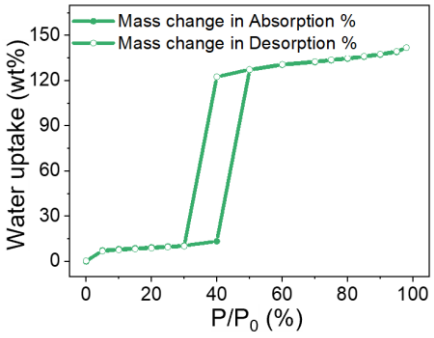

Figure S3 DVS sorption isotherms of synthesized MIL-101(Cr).

1.3. Comparison of surface area of MOF/wood composites.

Table S1 Comparison of the loading and surface area with MOF/wood composite with literatures.

Samples	MOF loading	SBET (m^2 g^{-1})	References
ZIF-L/Wood aerogel	36	6	[1]
CALF-20/Delignified wood	10	33.5	[2]
$Zn(MeIm)_2$/Delignified wood	4.1	37	[3]
AlBTC/Delignified wood	3.3	38	[3]
UiO-66-NH_2/Wood aerogel	29	46	[1]
ZIF-8/Wood aerogel	7.5	48.36	[4]
UiO-66/Delignified wood	11.1	56	[5]
ZIF-8/Delignified wood	12.1	131	[5]
$Cu_3(BTC)_2$/Delignified wood	10	136	[3]
MIL-100(Fe)/Delignified wood	25.4	170	[6]
MOF-199/Delignified wood	11.3	186	[5]
NH_2-MIL-53/Carbonizaed wood	52.2	185	[7]
CoNiP-C/ Carbonized wood	/	238.6	[8]
Co@C/Cabonized wood	/	280	[9]
ZIF-8/Basswood	4	16.896	[10]
ZIF-8/Beech wood	1.8	26	[11]
MIL-53(Al)/Pine	13.4	92	[12]
ZIF-8/Balsa wood	7.9	116	[13]
ZIF-8/Pine	13.4	236	[12]
MIL-101(Cr)/wood	17.08	316	This work

1.4 Characterizations of MOF/wood composites

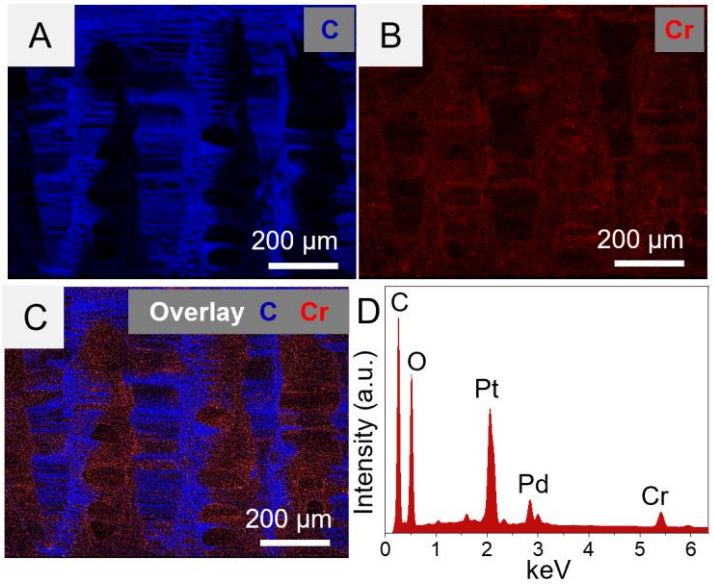

Figure S4 (A-C) Elemental maps of C (blue) and Cr (red) for MOF/wood composite, showing the successful loading and uniform dispersion of MOF in the wood scaffold. (D) Energy dispersive X-ray spectroscopy (EDX) spectra of MOF/wood composite.

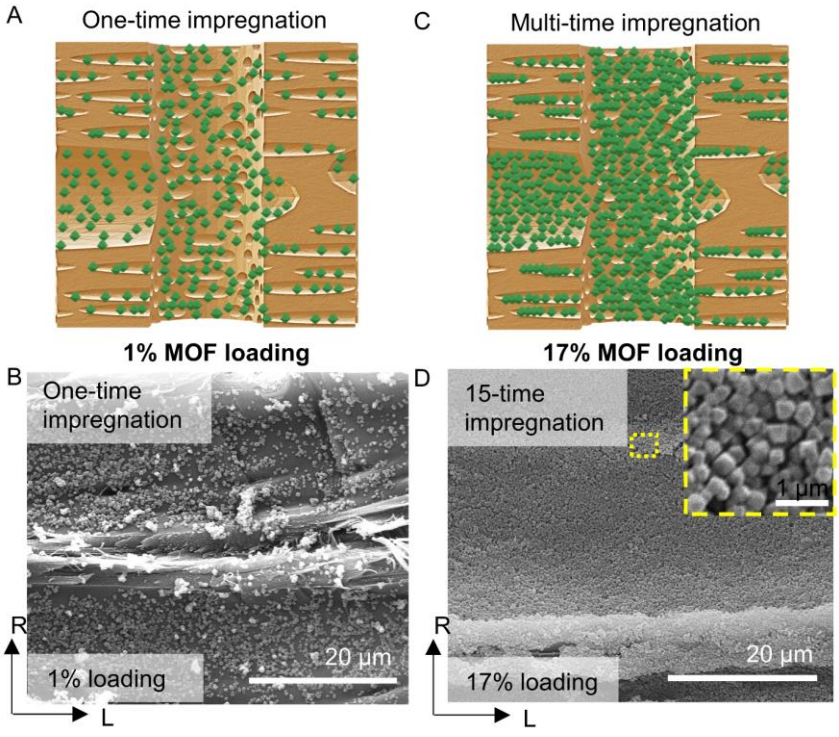

Figure S5 Influence of impregnation times. (A) Schematic representation and (B) SEM image of the MOF coating state on wood cell wall after one-time coating. (C) Schematic representation and (D) SEM image of the MOF coating state on wood cell wall after 15-time coating.

1.5. Porosity characterization

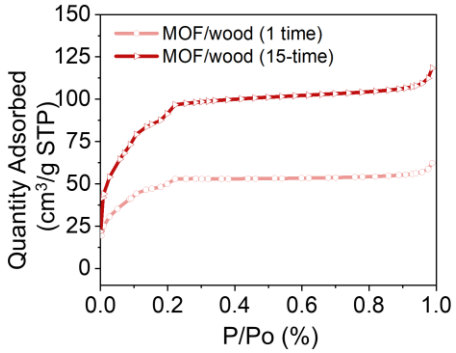

Figure S6 N_2 sorption curves of wood/MOF after one-time and 15-time coating.

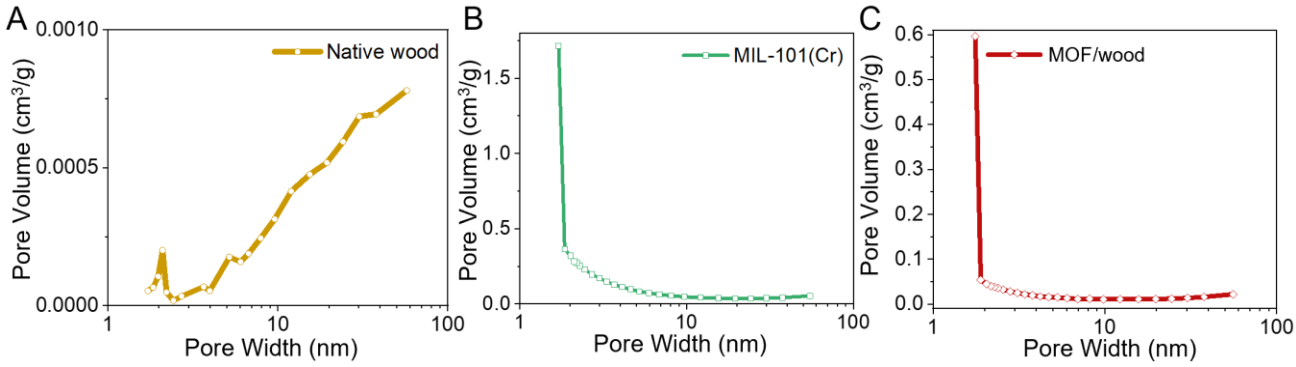

Figure S7 Pore volume distribution of native wood composite, MIL-101(Cr) and MOF/wood calculated from N_2 sorption.

Table S2 BET specific surface area of Native wood, MIL-101, and MOF/wood composite with one time coating and 15-time coating calculated from N_2 sorption.

Sample name	BET specific surfaces from N_2 sorption in $m^2\ g^{-1}$:
Native wood	0.343
MIL-101	2791
MOF/wood composite (1-time)	168
MOF/wood composite (15-time)	316

1.6. Mechanical performance.

Table S3 Ultimate tensile stress of different wood samples

Samples	Ultimate tensile stress (MPa)
Native wood	40.4 ± 11.6
Lasered wood	23.9 ± 7.3
MOF/wood composite	23.8 ± 3.6

2. Humidity regulation performance study.

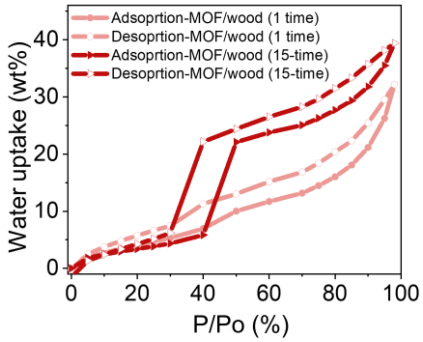

Figure S8 Water sorption isotherms of wood/MOF after one-time and 15-time coating.

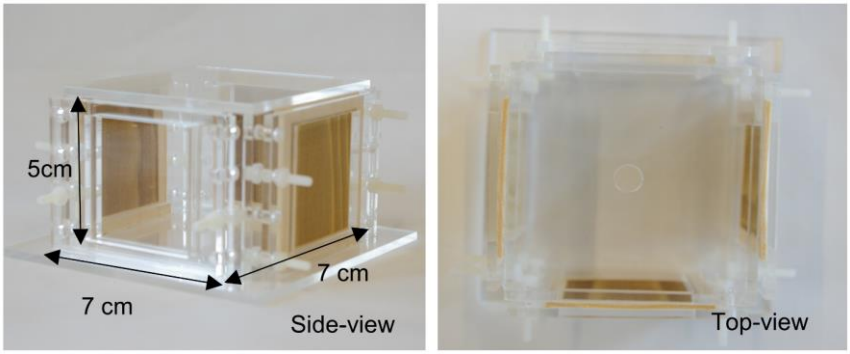

Figure S9 Images of the testing chamber with four sample windows.

3. Understanding Moisture Transport in Wood through Numerical Simulations.

The dimensions of the lasered holes and the volumetric ratio of porous wood to the lasered hole were estimated based on the SEM images in Figure 1. To provide a comprehensive view, the 2D results on the longitudinal section through the middle of the simulation domain are shown, with three lasered holes stitched together. Figure 5 depicts the simulated results exclusively in the adsorption process for enhanced clarity.

This study employs a two-phase moisture transport model for porous wood which considers both liquid water advection and water vapor diffusion.[14] For this model, two transport coefficients must be determined, water permeability for the liquid advection and water vapor diffusion coefficient. However, it is hard to measure them separately in a porous material at a given moisture condition. Measurements generally consider the moisture as a pure diffusion process; thus, the moisture diffusivity at different moisture contents can be determined, which includes transport of both liquid water advection and water vapor diffusion. This study utilizes the measured moisture diffusivity curve to determine water permeability and vapor diffusion coefficient. The black curve in Figure S11 was fitted based on the measured moisture diffusivity for native wood in the tangential direction summarized in literature.[15] However, no moisture transport coefficients for the MOF/wood composite were found in the literature. Therefore, we assumed the same water permeability for MOF/wood composite as for native wood and the corresponding results are presented in Figure S11. Notably, the diffusivity for MOF/wood composite generally exceeds that of native wood. The significant increase in moisture degree from 0.4 to 0.6 is attributed to the abrupt change in moisture content observed in the measured sorption isotherm (Figure 3A).

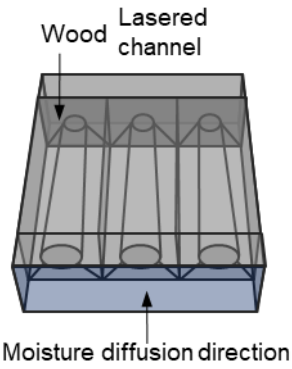

Figure S10 Illustration of the 3D model for numerical simulation.

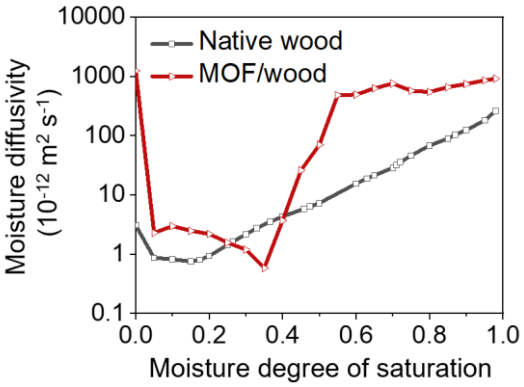

Figure S11 Moisture diffusivity in the tangential direction for the native wood and MOF/wood composite. Moisture diffusivity for native wood were measured in different studies and summarized in literature.[15] The

moisture diffusivity for the MOF/wood composite was calculated by using the same water permeability and water vapor diffusion coefficient as the native wood.

References

1. X. Y. Zhu, Z. X. Fan, X. F. Zhang and J. F. Yao, *J. Colloid Interface Sci.*, 2023, **629**, 182-188.
2. S. Roy, F. A. Philip, E. F. Oliveira, G. Singh, S. Joseph, R. M. Yadav, A. Adumbumkulath, S. Hassan, A. Khater and X. Wu, *Cell Reports Physical Science*, 2023, **4**, 101269.
3. S. N. Wang, C. Wang and Q. Zhou, *ACS Appl. Mater. Interfaces*, 2021, **13**, 29949-29959.
4. G. Zhu, C. L. Zhang, K. Q. Li, X. D. Xi, X. P. Zhang and H. Lei, *J. Porous Mater.*, 2022, **30**, 1171–1182.
5. Z. G. Wang, F. Y. Yin, X. F. Zhang, T. R. Zheng and J. F. Yao, *Sep. Purif. Technol.*, 2022, **293**, 121095.
6. X. Y. Zhu, M. J. Li, X. F. Zhang and J. F. Yao, *Microporous Mesoporous Mater.*, 2022, **342**, 112124.
7. Y. Gu, Y. C. Wang, H. M. Li, W. X. Qin, H. M. Zhang, G. Z. Wang, Y. X. Zhang and H. J. Zhao, *Chem. Eng. J.*, 2020, **387**, 124141.
8. R. R. Tian, C. Y. Duan, Y. Feng, M. J. Cao and J. F. Yao, *Energy & Fuels*, 2021, **35**, 4604-4608.
9. H. F. Qin, Y. Zhou, Q. Y. Huang, Z. Yang, R. Y. Dong, L. Li, J. H. Tang, C. Y. Zhang and F. Jiang, *ACS Appl. Mater. Interfaces*, 2021, **13**, 5460-5468.
10. Z. Wang, Y. He, L. Zhu, L. Zhang, B. Liu, Y. K. Zhang and T. Duan, *Mater. Chem. Phys.*, 2021, **258**, 123964.
11. K. K. Tu, B. Puertolas, M. Adobes-Vidal, Y. R. Wang, J. G. Sun, J. Traber, I. Burgert, J. Perez-Ramirez and T. Keplinger, *Adv. Sci.*, 2020, **7**.
12. A. Spiess, J. Wiebe, E. Iwaschko, D. Woschko and C. Janiak, *Mol Syst Des Eng*, 2022, **7**, 1682-1696.
13. X. F. Zhang, Z. G. Wang, L. Song and J. F. Yao, *Sep. Purif. Technol.*, 2021, **266**, 118527.
14. Z. D. Zhang, M. Thiery and V. Baroghel-Bouny, *Cem. Concr. Res.*, 2016, **89**, 257-268.
15. B. Time, *Hygroscopic moisture transport in wood*, Trondheim: Norwegian University of Science and Technology, 1998.